Personalization of Reaction-Diffusion Tumor Growth Models in MR Images: Application to Brain Gliomas Characterization and Radiotherapy Planning

Ender Konukoglu, Olivier Clatz, Hervé Delingette, Nicholas Ayache

Personalization of Reaction-Diffusion Tumor Growth Models in MR images: Application to Brain Gliomas Characterization and Radiotherapy Planning

Ender Konukoglu*, Olivier Clatz, Hervé Delingette and Nicholas Ayache

Asclepios Research Project, INRIA Sophia Antipolis – Méditerranée

*This work was partially supported by Microsoft Research Cambridge

Abstract

Reaction-diffusion based tumor growth models have been widely used in the literature for modeling the growth of brain gliomas. Lately, recent models have started integrating medical images, specifically anatomical and diffusion images, in their formulation. On the other hand, the adaptation of the general model to the specific patient cases has not been studied thoroughly yet. In this chapter we address this adaptation. This chapter is a short summary of the articles (Konukoglu 2009a), (Konukoglu 2009b) and the thesis (Konukoglu 2009c) that we have submitted recently. In the first part, we describe a parameter estimation method for reaction-diffusion tumor growth models using time series of medical (Magnetic Resonance) images. This method estimates the patient specific parameters of the model using the images of the patient taken at different successive time instances. In the second part of the chapter we focus on an application of the personalized models aimed to improve the tumor targeting in radiation therapy. Specifically we address the problem of limited visualization of medical images. We describe a method for extrapolating the invisible infiltration margins of gliomas in the MR images and the usage of these margins in constructing irradiation margins taking into account the growth dynamics of the tumor. Finally for both parts we show preliminary results demonstrating the power and the potential benefits of the personalization.

1. INTRODUCTION

Gliomas are neoplasms of glial cells which support and nourish the brain. These tumors have varying histopathological features and biological behavior showing different aggressiveness levels, from benign -grade I- to malignant -grade IV (Glioblastoma Multiforme). There has been a vast amount of research in mathematical modeling to describe the growth dynamics of these tumors (Byrne 2006, Cristini 2003, Frieboes 2007, Patel 2001, Stamatakos 2006, Zhang 2007). Lately, a specific type of macroscopic models, the reaction-diffusion models, received considerable attention from the literature in the attempt to link glioma growth models to medical images (Tracqui 1995,

Swanson 2000, Clatz 2005, Jbabdi 2005, Hogea 2007, Mandonnet 2008). These recent models integrate information coming from medical images, specifically through anatomical and diffusion images, in their formulation. This integration is crucial for the transfer of mathematical models to the clinical applications since medical images are conventionally used for diagnosis and patient follow-up in the clinical routine. One of the biggest challenges in this transfer is the automatic adaptation of mathematical models to the patient based on images. In this chapter, first we address the problem of adapting the recent reaction-diffusion models to specific patient cases using time series of medical (Magnetic Resonance - MR) images (Konukoglu 2009a). Following this, we address the question of retrieving relevant information for radiotherapy planning from the personalized reaction-diffusion models (Konukoglu 2009c).

1.1 Reaction-Diffusion Models

Reaction-diffusion models describe the evolution of gliomas via proliferation of tumor cells and infiltration of the surrounding healthy tissue. The building block of these models is the reaction-diffusion type partial differential equations of this form:

$$\frac{\partial u}{\partial t} = \nabla \cdot \left(\mathbf{D}(\mathbf{x}) \nabla u \right) + \rho u (1-u), \ \mathbf{D} \nabla u \cdot \mathbf{n}_{\partial \mathbf{\Omega}} \ (1)$$

where u represents the tumor cell density, D is the local diffusion tensor (i.e. symmetric positive definite 3x3 matrix), ρ is the proliferation rate, Ω is the brain domain and $\partial \Omega$ represents the boundaries of the brain. The two terms on the right hand side correspond to the two phenomena described by the model: the diffusion term $\nabla \cdot \left(\mathbf{D} \nabla u \right)$ models the migration of tumor cells within the brain tissue and the reaction term $\rho u(1-u)$ models the proliferation of tumor cells.

Different models proposed in the literature mostly differ by the construction of the D tensor and the form of the proliferation term (Tracqui 1995, Swanson 2000, Giese 1996, Clatz 2005, Jbabdi 2005, Hogea 2007). In this chapter we concentrate on the personalization of the growth models proposed in (Clatz 2005) and (Jbabdi 2005). However, the methods explained in this chapter are independent from the exact construction of the tensor and can be applied to both of these formulations as well as to other reaction-diffusion models. The two aforementioned models are

based on Equation (1) and they construct the diffusion tensor D as follows:

$$\mathbf{D(x)} = \begin{cases} d_g\mathbf{I}, & \mathbf{x} \in \text{gray matter} \\ f(d_w, \mathbf{D_{water}}), & \mathbf{x} \in \text{white matter} \end{cases} \quad (2)$$

The choice of the function f is defined differently in the two models:

$$f = \begin{cases} d_w\mathbf{D_{water}}, & \text{(Clatz 2005)} \\ \mathbf{V(x)}\left[\text{diag}\left(e_1(x)d_w, d_g, d_g\right)\right]\mathbf{V(x)^T}, & \text{(Jbabdi 2005)} \end{cases}$$

where d_w is the diffusion rate in the white matter (Clatz 2005) or along the white matter fiber tracts (Jbabdi 2005), d_g is the diffusion rate in the gray matter, $D_{water} = V\Lambda V^T$ is the diffusion tensor of water molecules at point $\mathbf{x}$ with e_1 being its highest eigenvalue.

1.2 Image-Guided Model Personalization

Once the mathematical model describing the general dynamics of the tumor growth process is created, the personalization is defined as the estimation of the model parameters based on the observations. The image-guided personalization focuses on determining the reaction-diffusion parameters, the diffusion tensor D *(d_w and d_g)* and the proliferation rate ρ, based on the observed evolution of the tumor in the time series medical images. The difficulty in this estimation is due to the sparsity of the available information. The reaction-diffusion models describe the temporal evolution of *tumor cell densities* while in the images we only observe the evolution of the *tumor delineation* which is assumed to correspond to an iso-density contour (Burger 1988) as shown in Figure 1. Therefore, reaction-diffusion models are not directly applicable for the estimation problem.

[FIGURE 1 TO BE PLACED HERE – images, visibility problem]

The problem of parameter estimation in the context of tumor growth models is a rather unexplored problem. A first attempt was made by Tracqui *et al.* in (Tracqui 1995) where they optimized the parameters of their model by comparing the area of the tumor observed in CT images at different times and the area of the simulated tumor. The drawback of this approach was to use tumor cell densities requiring an initialization of the density distribution throughout the brain while these densities are not observable in the images (again, we observe tumor delineations). More

recently, in (Hogea 2008), Hogea *et al.* have optimized their parameters using two different methods: by comparing locations of some manually placed landmarks with the model generated ones and by comparing tumor cell densities extracted from the images and generated by the model. In addition to the parameters of the reaction-diffusion model they optimize the parameters of their mechanical model as well. The use of tumor cell densities in the optimization process has the same problems as the previously mentioned method, they are not observable. The landmarks on the other hand, seems to be a promising approach, however, the parameter values obtained in this approach depend on the assumed coupling between the mechanical and the patho-physiological model. The resulting parameters are not purely inherent to the tumor. Recently Swanson *et al.* in (Swanson 2008) proposed a parameter estimation method for the diffusion process in petri-dish experiments, which is consistent with the observed information in the images as it uses the tumor boundaries rather than tumor cell densities. They have derived analytical approximations for the evolution of the tumor delineation for 2 dimensional circular growth. Using the formulation for the tumor delineation they have estimated the diffusion coefficient for the petri-dish experiments. The difficulty one would encounter if one wants to apply this method to medical images is that the method assumes radial symmetric growth which is not the case in the brain (*in-vivo*). Moreover, the existence of a reaction term results in a different evolution than pure diffusion.

In this chapter, we explain and analyze a parameter estimation method for reaction-diffusion based tumor growth models using time series of MR images. The method is based on the evolution of the tumor delineation rather than tumor cell densities and in this respect it is consistent with the observations in the images. It also takes into account tissue inhomogeneities, fiber structures and the real geometry of both the patient's brain and the tumor while remaining consistent with the image information. We also present preliminary promising results on 2 sets of patient data.

1.3 Infiltration Extent of Gliomas and Constructing Model based Irradiation Margins

For the diagnosis and the therapy of gliomas, clinicians rely on medical images, such as Magnetic Resonance (MR) and Computed Tomography (CT) images, which show the mass part of

the tumor. Current imaging techniques are not able to expose the low density infiltration (Tovi 1994, Tracqui 1995, Swanson 2004) posing a problem for the experts in outlining the whole tumor and in delineating its extent (see Figure 1). In radiotherapy, this problem of visualizing low density infiltration is addressed by outlining a constant margin of 2 cm around the visible tumor boundary for irradiation and assuming the whole tumor infiltration is contained within this region (Seither 1995, Kantor 2001). This approach does not take into account the infiltration dynamics of gliomas, particularly the higher motility of tumor cells in white matter compared to gray matter (Giese 1996). As a result, the irradiation region ignoring these dynamics might not reach the full extent of the tumor infiltration in white matter and irradiate healthy gray matter. The importance of this problem was shown by Swanson *et al.* in (Swanson 2002) where they compare the visible part of the tumor with the extent of the invisible infiltration for virtual tumors grown by reaction-diffusion models. Personalized tumor growth models can offer solutions to this problem by integrating clinical information and theoretical knowledge about tumor cell dynamics. In this chapter we describe a new formulation which aims to solve the problem of estimating tumor cell density distribution beyond the visible boundary of gliomas in the images. Starting from the tumor delineation either found by a segmentation algorithm or manually drawn by an expert it produces a map of possible tumor infiltration. It uses the anatomical MR images and diffusion tensor images (DTI) to suggest irradiation margins taking into account the growth dynamics. We then use the extrapolated infiltration extents to create variable irradiation margins. The potential benefits of such margins in targeting tumor cells are also described.

2. METHODS

2.1 Parameter Estimation and Model Personalization

The reaction-diffusion model given in Equations (1) and (2) describes the temporal evolution of local tumor cell densities. In order to solve the parameter estimation problem we need a formulation consistent with the image: it should model the evolution of the tumor delineation rather than the evolution of the cell densities. In this section, first we present the traveling time

formulation for tumor delineation which captures the same growth dynamics as the reaction-diffusion models while remaining consistent with the image information. Then we formulate the parameter estimation problem as an optimization problem based on the MR images using the traveling time formulation.

2.1.1 Traveling Time Formulation for Tumor Delineation

The asymptotic properties of the reaction-diffusion equations under certain conditions allow us to construct a formulation for the tumor delineation as described above, *the traveling time formulation*. Reaction-diffusion equations and their asymptotic properties have been well studied in the literature (Aronson 1978, Ebert 2000). The property on which we base our derivation is the existence of *traveling wave solutions* of the reaction-diffusion equations and the convergence of different initial conditions to these solutions in time.

The constant coefficient case of Equation (1) admits a traveling wave solution in the infinite cylinder given as

$$u(x,t) = u(\mathbf{n} \cdot \mathbf{x} - vt) = u(\xi),$$

where v is the speed of the wave (front of the u distribution), $\boldsymbol{n}$ is the direction of motion of the wave and $\xi = \mathbf{n} \cdot \mathbf{x} - vt$ is the moving frame of the traveling wave. There are two important characteristics of the reaction-diffusion equations and the traveling wave solutions that are very useful for our derivation:

- For the traveling wave solution, all iso-density contours of the distribution u move with the same speed v.

- Any compact support initial condition $u(\boldsymbol{x},0)$ of the reaction-diffusion equation (1) converges to the traveling wave solution in time (see Figure 2). Therefore, the traveling wave solution serves as a good approximation for a certain class of solutions of the reaction-diffusion equation.

Based on these two characteristics we can model the evolution of the tumor delineation through the speed of the traveling wave.

[PLACE FIGURE 2 – convergence of the reaction-diffusion initializations to the traveling wave]

The asymptotic speed v of the traveling wave solution is given as a function of the model parameters

$$v = 2\sqrt{\rho \mathbf{n'Dn}} \text{, (3)}$$

where this speed is defined in the infinite cylinder under the constant coefficient assumption. In the case of the tumor modeling the shape of the tumor is arbitrary and the model coefficients can be spatially and temporally varying. Therefore, the above assumptions should be relaxed. Under the assumptions that the tumor delineation is planar and coefficients are constant within each image voxel, we can write a preliminary traveling time formulation for the tumor delineation using v:

$$2\sqrt{\rho}\sqrt{\nabla T' \mathbf{D} \nabla T} = 1 \text{, (4)}$$

$$T(\mathbf{x}) = T_0 \; \forall \mathbf{x} \in \Gamma \text{, (5)}$$

where $T(\mathbf{x})$ is an implicit time function representing the time when the tumor delineation passes through the point $\mathbf{x}$. Equation 5 represents the Dirichlet type boundary condition stating that the tumor delineation reaches the surface Γ in T_0 time since its emergence. The value of T_0 is the absolute time value and it is not known from the images. However, we do not need to know this value in order to evolve the tumor delineation with the model given in Equation (4). The formulation given by Equations (4) and (5) is in a sense a first order approximation. It does not take into account the convergence rate of the initial distribution u to the traveling wave solution - see Figure 2 - and the effect of the curvature of the tumor delineation on its speed. These effects can be included, leading to the final traveling time formulation for the tumor delineation as follows (Konukoglu 2009a)

$$\left\{\frac{4\rho T - 3}{2T\sqrt{\rho}} - 0.3\sqrt{\rho}\left(1 - e^{-|\kappa_{eff}|/(0.3\sqrt{\rho})}\right)\right\}\sqrt{\nabla T' \mathbf{D} \nabla T} = 1 \text{ (6)}$$

$$\kappa_{eff} = \nabla \cdot \frac{\mathbf{D} \nabla T}{\sqrt{\nabla T' \mathbf{D} \nabla T}}, \; T(\mathbf{x}) = T_0 \; \forall \mathbf{x} \in \Gamma \text{ ,}$$

where the term $(4\rho T - 3)/(2T\sqrt{\rho})$ is the effect of the tumor rate of convergence and the term with κ_{eff} is the effect of the tumor delineation's curvature on its evolution. The traveling time formulation

given in Equation (6) describes the evolution of the tumor delineation in the MR images based on the same growth dynamics as the reaction-diffusion models. In the formulation given in Equation (6) we notice the T dependence of the equation. This means that the value of T_0 becomes important for the simulation. As we have noted this value is cannot be known in the clinical routine this seems to pose a problem. However, we solve this problem by treating this value as another model parameter to be optimized for.

In Figure 3 we show an example evolution simulated using the traveling time formulation to show that it captures the same growth dynamics as the reaction-diffusion model given in Equations (1) and (2). We compare the evolution of a synthetic tumor delineation simulated by the reaction-diffusion model (in white) and by the traveling time formulation (in black). In the case of the reaction-diffusion model the synthetic delineation is obtained by thresholding the tumor cell density distribution, which would not be available in patient cases.

[PLACE FIGURE 3 – comparison of the traveling time with reaction-diffusion]

2.1.2 The Parameter Estimation Formulation

Since we have linked the reaction-diffusion model and the evolution of the tumor delineation through traveling time formulation, we can formulate the parameter estimation problem using this link. In the reaction-diffusion model given in Equations (1) and (2) there are three different parameters: d_w, d_g and ρ. In addition to these, in the previous section we added another parameter T_0 in the traveling time formulation as a result of integrating the convergence characteristics of the reaction-diffusion solutions. This results in 4 parameters to estimate for. Our aim is to optimize these parameters such that the evolution simulated using the traveling time formulation best matches the real evolution observed in the time series of MR images.

As the first step we define a discrepancy measure between the simulated tumor evolution and the observed one for a given set of parameters. Minimizing this discrepancy then would provide us the optimum model parameters. Our strategy in defining this discrepancy is to use the symmetric surface distances between the simulated and the real delineations and also add a criterion regarding

8

the initial size of the tumor in the first acquired image. The resulting criterion becomes a quadratic measure as follows:

$$C(d_w, d_g, \rho, T_0) = \sum_1^{N-1} \{\text{dist}(\Gamma_i, \hat{\Gamma}_i)\} + v_{\min} |T_{\min} - T_0|^2 \quad (7)$$

$$\hat{\Gamma}_i = \{\mathbf{x} \mid T(\mathbf{x}) = T_0 + \Delta t_i\} \text{ with } T(\mathbf{x}) = T_0 \ \forall \mathbf{x} \in \Gamma_0 \quad (8)$$

$$v_{\min} = 0.1 \sqrt{\rho \mathbf{n}_{\max}' \mathbf{D}(\mathbf{x}_{\min}) \mathbf{n}_{\max}}, \ T_{\min} = T(\mathbf{x}_{\min}) \quad (9)$$

where N is the number of images, Γ_i is the delineation enclosing the tumor in the ith image, dist() is the symmetric distance between two surfaces, Δt_i is the time difference between the ith and the first MR image, x_{min} is the point where the simulated T reaches its minimum and $\mathbf{n}_{\max}$ is the principal eigenvector of $\mathbf{D}(x_{min})$. In Equation (7) the summation measures the distance between the simulated and the real observations. This is obtained by running the traveling time formulation outwards starting from the delineation of the tumor obtained in the first image and comparing the corresponding simulated and observed delineations for the other images. The other term in the same equation, $v_{\min} |T_{\min} - T_0|^2$, takes into account the size of the visible tumor in the first image and quantifies the coherency of this size with the model parameters. We compute this value by simulating the traveling time evolution within the tumor delineation in the first image and compare the minimum T value obtained with the T_0 parameter. If all the parameters of the model are coherent with the observations then this term should equal to zero.

We define the parameter estimation problem as the minimization of the error measure defined in Equation (7). Different optimization algorithms can be used for this purpose. Since the gradients of C are not trivial to find analytically we prefer to use a general algorithm which approximates the gradient directions. In this work we use the algorithm proposed by Powell in (Powell 2001) which finds the gradient directions by fitting quadratic surfaces to the underlying minimization surface. Computation times depend on the size of the tumor and the number of images. As an example for a high grade glioma with a time series of 4 images of size (256x256x53) the minimization takes around 50 minutes on a 2.4 GHz Intel Pentium machine with 1 Gb of RAM.

In Figure 4 we provide an example showing the inputs and the outputs of the parameter estimation method.

[PLACE FIGURE 4 – inputs and the outputs of the parameter estimation method]

2.2 Extrapolating Infiltration Extent and Adaptive Irradiation Margins

In the previous section we presented a method to personalize the reaction-diffusion type tumor growth models using the MR images of the patient. Here we assume that we have the personalized model and we present a method to extrapolate the cell density distribution of the tumor beyond its delineation in the image. This method produces a map of possible tumor infiltration that is not visible in the image. Then using this map we describe a method for constructing variable irradiation margins taking into account the growth dynamics of the tumor.

2.2.1 Extrapolating Invisible Infiltration Extents of Gliomas

In order to formulate the extrapolation method first we need an imaging model for the gliomas. We assume that this imaging process can be modeled using a Heaviside function as done in (Tracqui 1995) and in (Swanson 2000). The imaging function Im is given as

$$\text{Im}(u(\mathbf{x},t)) = \begin{cases} 1 \ if \ \ u \ge u_0 \\ 0 \ if \ \ u < u_0 \end{cases}, (10)$$

we define 1 as enhanced, 0 as non-enhanced regions in the image and u_0 is the tumor cell density threshold of the imaging modality. This simplistic model assumes that the delineations in the images correspond to an iso-density contour of the tumor cell density distribution. A more general imaging function can be used and similar ideas presented below would be applicable. Based on this definition the problem of extrapolating cell density distribution of a tumor beyond its delineation in the image is defined as

$$\tilde{u}(\mathbf{x}) \approx u(\mathbf{x},T_0) \ \forall \mathbf{x} \in \{\mathbf{x} \,|\, \text{Im}(\mathbf{x}) = 0\}, (11)$$

where $\tilde{u}$ approximates the actual tumor distribution at a time instant T_0. Unlike the forward modeling of the tumor growth, the construction of the approximation $\tilde{u}$ is a static problem and it *does not involve the time evolution* of the tumor. Moreover, in the clinical situations, the value of

T0, which indicates the time elapsed between the emergence of the tumor and the image ***acquisition*** is not available.

The ability to personalize reaction-diffusion models give us the opportunity to construct $\tilde{u}$ for patient images. The asymptotic properties of the reaction-diffusion equations explained in Section 2.1 allow us to write the following formulation

$$\frac{\sqrt{\nabla\tilde{u}\cdot(\mathbf{D}\nabla\tilde{u})}}{\sqrt{\rho\tilde{u}(1-\tilde{u})}} = 1, \tilde{u}(\Gamma) = u_0. \text{ (12)}$$

In this equation Γ is the tumor delineation in the image either found by a segmentation algorithm or drawn manually. For the derivation of this formulation we ask the reviewer to refer to (Konukoglu 2009c). Equation (12) provides us a gradient relationship for $\tilde{u}$. In order to solve this equation we start from the enhanced part of the tumor in the image and sweep the brain tissue outwards computing possible tumor cell density values at every point. Since the equation is an anisotropic Eikonal equation and such a solution it can be rapidly constructed using Fast Marching methods suitable to the exact form of the equation (Konukoglu 2007). In Figure 5, for a virtual tumor grown by the reaction-diffusion model, we demonstrate the visible part of the tumor, the invisible infiltration and the reconstructed tumor cell density based only on the visible part of the tumor and personalized parameters. We observe the similarity between the distributions.

[PLACE FIGURE 5]

2.2.2 Adaptive Irradiation Margins

In conventional radiotherapy the irradiation margins are constructed based on the tumor geometry visible in the medical images. The margin takes into account the enhanced area of the tumor in the image plus a constant margin around the delineation to deal with the low cell density infiltration (Kantor 2001). This approach assumes that the tumor cells would diffuse within the brain tissue homogeneously around the visible tumor. It does not take into account the growth dynamics of the tumor especially the differential motility (Giese 1996).

The extrapolation method presented in the previous section gives us a map of possible tumor

infiltration that is not visible in the images. We can use this to construct irradiation margins adapted to this map. Our strategy is to first construct the conventional constant margin irradiation region M_c and then create the adapted margins M_v by molding M_c such that M_v takes into account the infiltration extent constructed as explained in the previous section. We refer the reader to (Konukoglu 2009c) for the details of this construction. In Figure 6 we demonstrate the two margins, the constant and the variable ones. For a virtually grown tumor we show the visible part of the tumor, its invisible infiltration and the constant and the variable irradiation margins constructed based on its visible part.

[PLACE FIGURE 6 – variable irradiation margin]

3. RESULTS

3.1 Parameter Estimation and Model Personalization

The evaluation of parameter estimation for tumor growth models using real patient images is not easy because we do not have access to the real values of the parameters. The real values could be found using microscopic *in-vivo* analysis however, up to the best of our knowledge such a study has not been performed yet. In this work we perform an indirect evaluation for the proposed parameter estimation method using patient images. For a given patient dataset, we estimate the parameters using all but the image taken at the last time point. Then using the estimated parameters we simulate the evolution of the tumor delineation for the time elapsed between the 2 last images. We then compare the evolution predicted using the estimated parameters and the travelling time formulation with the one observed in the last image. The correlation between the prediction and the observed delineation provides us with a qualitative evaluation of the estimated parameters.

In the parameter estimation process it is shown in (Konukoglu 2009a) that estimating all the parameters of the model independently using the evolution of the tumor delineations in the images results in non-unique solutions. Therefore in this study we fix the proliferation rates ρ of the tumors to the values suggested in the literature. We only estimate for the diffusion rates and the initial time estimates. In fixing the value of ρ we assume that this value can be estimated based on the biopsy

results and microscopic analysis using the relation between the mitotic index (MI) and the labelling index (LI) (Johannessen 2006).

As a preliminary step we use two patient datasets which include anatomical and diffusion tensor MR images. The dataset for the first patient, who suffers from a high grade glioma (Glioblastoma Multiforme), includes T1-post gadolinium MR images (with the resolution of 0.5x0.5x6.5 mm3) at three successive different time points and diffusion tensor MR image (with the resolution of 2.5x2.5x2.5 mm3) taken at the second time point. The second patient suffers from a low grade glioma (second grade astrocytoma) and the dataset for this patient includes T2 flair MR images (with the resolution of 0.5x0.5x6.5 mm3) at 5 successive time points and the DT-MRI image (with the resolution of 2.5x2.5x2.5 mm3) taken at the first time point. For both cases the tumor boundaries were manually delineated by an expert in each image separately.

[PLACE FIGURE 7 – high grade patient]

[PLACE FIGURE 8 – low grade patient]

The images used to estimate parameters, the estimated parameters and the predicted evolution of the tumor delineations along with the real delineations are given in Figures 7 and 8. In the images in both Figures, first we show the anatomical images at the time of detection and the intermediate images used in the parameter estimation. On the intermediate images we also plot the manual delineations for the underlying image (white contour) and the simulated evolution of the tumor delineation with the estimated parameters (dark contour) obtained in the course of estimation. Following this we start from the last image (in time) used in the parameter estimation and predict the evolution of the tumor delineation until the acquisition of the final image (which was not used in the estimation). In the corresponding images we show the anatomical MR image taken at the last time point showing the final state of the tumor along the tumor delineation predicted using the estimated parameters drawn as the dark contour. In the accompanying tables we provide the values of the estimated parameters.

We observe in Figure 7(c) that the prediction of the tumor delineation is in very good

agreement with the final state of the tumor. In the case of the low grade tumor shown in Figure 8,

the correlation between the predicted tumor delineation and the final state of the tumor is in line

with our previous arguments. We observe that the slow evolution of the tumor is well captured by

the estimated parameters. For the proliferation rate we pick a lower value than the one in the

previous case since it is a lower grade tumor.

3.2 Extrapolating Infiltration Extent and Adaptive Irradiation Margins

In this section we assess the quality of the extrapolation method and the method for

constructing the variable, adaptive irradiation margins. In order to understand the potential benefits

of extrapolating the infiltration extents of gliomas and constructing irradiation margins adapted to

these results we perform experiments on synthetic images. We create a dataset of virtually grown

tumors using the reaction-diffusion models where the tumors are grown in the MR images of a

healthy subject ($1\times1\times2.6$ mm^3 resolution). Different tumors in the dataset are created using different

model parameters and different seed points in the brain. For each tumor we construct synthetic

images using the Im() function given in Equation 10 with u_0=0.4, value consistent with (Tracqui

1995). We assume that the detection and the first image acquisition take place when the average

diameter of the visible tumor reaches 1.5 cm. After the detection for each tumor we construct a

synthetic image every 50 days for 1 year (8 images in total). An example of the created synthetic

image with the synthetic tumor is shown in Figure 6. For the tumors in the dataset we construct the

constant and the variable irradiation margins based on their visible parts in the images. Since for the

virtual tumors, the cell density at every location is known – even if the image does not show tumor

at that point – we carry out a quantitative comparison. We geometrically compare these margins

based on two criteria:

1. *R*: number of tumor cells **not** targeted and

2. *Vol*: volume of healthy tissue targeted by the irradiation margin.

In order to compute these values we follow the values given in (Tracqui 1995) we assume that a

voxel of 1x1x2.6 mm^3 can hold a maximum of 9.1x10^4 tumor cells. At the time of detection of high grade gliomas, isolated tumor cells can be found in any region in the brain. Therefore, there is no completely healthy brain. In order to compute the *Vol* value we need to define "healthy tissue". In this work we define a voxel to be healthy if there are on the average less than 1 tumor cell in it. In Figure 9 for a synthetic tumor we show the comparison between the constant and the variable irradiation margins. We plot the *R* vs. time and *Vol* vs. time graphs. We observe that the variable irradiation margins adapted to the extrapolated infiltration extents targets more tumor cells and less healthy tissue.

[PLACE FIGURE 9 – showing the R vs. time and Vol vs. time graph for an example tumor. Give the parameter values in the caption.]

The experiments presented above use synthetic images and virtually grown tumors. Validating the presented methods on real images would require the knowledge of tumor cell density distributions throughout the brain. This could be obtained with post-mortem analysis or with animal models. This would be the topic of a future study.

4. CONCLUSION

In this chapter we presented methods to personalize reaction-diffusion type tumor growth models in MR images. Our aim was to bridge the gap between the mathematical tumor growth models and the clinical applications. In this spirit, first we focused on a method for personalizing the generic reaction-diffusion growth models based on time series of MR images. The method described the evolution of the tumor delineation in the images based on the growth dynamics captured by the reaction-diffusion models. Based on this formulation it optimized for the model parameters such that the resulting simulations best matches the observed evolution of the tumor boundaries in the MR images. The results shown in Section 3 demonstrated promising preliminary findings.

As a second part, we presented an application of personalized tumor growth models for radiotherapy to demonstrate clinical relevance of the personalization process. We constructed the

possible tumor infiltration map of gliomas starting from their visible delineation in the MR images. Using this map we proposed variable irradiation margins which are adapted to the modeled growth dynamics of the observed tumor. We also showed potential benefits of such variable irradiation margins compared to constant ones.

Although a preliminary validation was performed a thorough validation remains to be done on animal models and post-mortem analysis.

5. ACKNOWLEDGEMENTS

VI. REFERENCES

(Aronson 1978) Aronson, D., Weinberger, H. 1978. Multidimensional nonlinear diffusion arising in population genetics. *Advances in Mathematics* 30

(Byrne 2006) Byrne, H.M., Owen, M.R., Alarcon, T., Murphy, J. and Maini, P.K., 2006. Modelling the response of vascular tumours to chemotherapy: a multiscale approach. *Mathematical Models and Methods in Applied Sciences,* 16:1219-41

(Clatz 2005) Clatz, O., Sermesant, M., Bondiau, P-Y. *et al.*2005. Realistic simulation of the 3D growth of brain tumors in MR images coupling diffusion with biomechanical deformation. *IEEE TMI* 24

(Cristini 2003) Cristini, V., Lowengrub, J., Nie, Q. 2003. Nonlinear simulation of tumor growth. *Journal of Math. Bio.* 46

(Saarloos 2000) Saarlos, W.V., Ebert, U., 2000. Front propagation into unstable states: universal algebraic convergence towards uniformly translating pulled fronts. *Pysica D: Nonlinear Phenomena* 146.

(Frieboes 2007) Frieboes, H., Lowengrub, J., Wise, S., *et al.* 2007. Computer simulation of glioma growth and morphology. *NeuroImage* 37:S59-S70.

(Hogea 2007) Hogea, C., Davatzikos, C. and Biros, G. 2007. Modeling glioma growth and mass effect in 3D MR images of the brain. *LNCS Proceedings of MICCAI* 4791:642-50

(Hogea 2008) Hogea, C., Davatzikos, C. and Biros, G. 2007. An image-driven parameter estimation problem for a

reaction-diffusion glioma growth model with mass effects. *Journal of Math. Biol.* 56:793-825.

(Jbabdi 2005) Jbabdi, S., Mandonnet, E., Duffau, H., *et al.* 2005. Simulation of anisotropic growth of low-grade gliomas using diffusion tensor imaging. *Magnetic Reson. in Med.* 54

(Johannessen 2006) Johannessen, A.L., Torp, S.H. 2006. The clinical value of Ki-67/MIB-1 labeling index in human astrocytomas. *Pathol. Oncol. Res.* 12:143-47.

(Kantor 2001) Kantor, G.., Loiseau, H., Vital, A., Mazeron, J., 2001. Descriptions of GTV and CTV for radiation therapy of adult glioma, *Cancer Radiotherapy* 5:571-80.

(Konukoglu 2007) Konukoglu, E., Sermesant, M., Clatz, O., et al. 2007. A recursive anisotropic fast marching approach to reaction diffusion equation : Application to tumor growth modeling. *LNCS Proceedings of IPMI*. 4584

(Konukoglu 2009a) Konukoglu, E., Clatz, O., Menze, B. H., *et al.* 2009. Image guided personalization of reaction-diffusion type tumor growth models using modified anisotropic eikonal equations. *IEEE TMI in press.*

(Konukoglu 2009b) Konukoglu, E., Clatz, O., Bondiau, P.-Y., Delingette, H. and Ayache, N., 2009. Extrapolating Glioma Invasion Margin in Brain Magnetic Resonance Images: Suggesting New Irradiation Margins, *Submitted to Med. Im. Anal.*

(Konukoglu 2009c) Konukoglu, E. 2009. Modeling Glioma Growth and Personalizing Growth Models in Medical Images, *PHD Thesis - Université de Nice - Sophia Antipolis.*

(Mandonnet 2008) Mandonnet, E., Pallud, J., Clatz, O., *et al.* 2008. Computational modeling of the WHO grade II glioma dynamics: principles and applications to management paradigm. *Neurosurgery Review* 31:263-69

(Patel 2001) Patel, A., Gawlinski, E., Lemieux, S., Gatenby, R. 2001. A cellular automaton model of early tumor growth and invasion. *Journal of Theo. Bio.* 213.

(Powell 2001) Powell, M., 2001. UOBYQA: Unconstrained optimization by quadratic approximation. *Math. Prog. Ser. B* 92.

(Stamatakos 2006) Stamatakos, G., Antipas, V., Uzunoglu, N. 2006. A spatiotemporal, patient individualized simulation model of solid tumor response to chemotherapy in vivo. *IEEE Tran. Bio. Med. Eng.* 53:1467-77

(Swanson 2000) Swanson, K.R. , Alvord, E.C. and Murray, J.D. 2000. The modelling of diffusive tumours. *J. Bio. Sys.* 3

(Swanson 2002) Swanson K.R., Alvord, E.C. and Murray J.D. 2002. Virtual brain tumours (gliomas) enhance the reality of medical imaging and highlight inadequacies of current therapy. *British Journal of Cancer* 86.

(Swanson 2004) Swanson K.R., Alvord, E.C. and Murray J.D. 2004. Dynamics of a model for brain tumors reveals a small window for therapeutic intervention. *Discrete and Continuous Dynamical Systems-Series B* 4:289-95.

(Swanson 2008) Swanson, K. 2008. Quantifying glioma cell growth and invasion *in vitro. Math. Comp. Model* 47:638-48.

(Tovi 1994) Tovi., M., Hartman, M., Lilja, A., and Ericsson, A. 1994. MR imaging of cerebral gliomas. Tissue component analysis in correlation with histopathology of whole-brain specimens. *Acta Radiologica* 35:495-505.

(Tracqui 1995) Tracqui, P., Cruywagen, G., Woodward, D., *et al.* 1995. A mathematical model of glioma growth: the effect of chemotherapy on spatio-temporal growth. *Cell Proliferation* 28.

(Zhang 2007) Zhang, L., Athale, C.A. and Deisboeck, T.S. 2007. Development of a three-dimensional multiscale agent-based tumor model: simulating gene-protein interaction profiles, cell phenotypes and multicellular patterns in brain cancer. *Journal of Theo. Bio.* 244:96-1077.

Captions

Fig1: (Left) T2-weighted and (Middle) T1-weighted post-gad MR images showing a high grade glioma. The bulk tumor and the infiltrated edema are the enhanced regions in the left and the middle images respectively. (Right) Hypothetical distribution of tumor cell density is a smooth transition starting from the bulk tumor extending beyond the edema.

Fig2: Any initial condition with compact support when evolved with reaction-diffusion equations (in the infinite cylinder and constant coefficients) converges to the traveling wave solution. (Left) A Heaviside initialization is evolved in time. (Middle)We plot the distribution at different times on the moving frame. (Right) The traveling wave solution has an asymptotic speed shown in dashed curve however, when we observe the speed of the tumor front (u=0.5 iso-density contour) we notice the low rate of convergence (solid curve). An approximation of the tumor front's speed including time convergence and curvature we get a better approximation (point-dashed curve).

Fig3: Comparison between the reaction-diffusion model and the Eikonal Approximation: The temporal evolution of the iso-density contour is demonstrated for a synthetic tumor. Contours are shown for days 400, 600, 800, 1000 and 1200 from the innermost to outermost respectively. The synthetic tumor is virtually grown using the reaction-diffusion model. White contours are obtained by thresholding the tumor cell densities at u = 0.4 for the respective day values (400-600-800-1000-1200). Then in order to simulate the evolution of the iso-density contour (assumed to correspond to tumor delineation in real images) starting from day=400, without the knowledge of the tumor cell density distribution we use the traveling time formulation. Black curves are the contours we obtain at days 600 (2nd innermost) to 1200 (outermost). The tumors were grown in the images of a healthy subject for whom we also have the DT-MRIs. Parameters: (dw = 0.25 mm2/day,dg = 0.01 mm2/day, ρ = 0.012 day−1). The figure is Copyright © 2009 IEEE.

Fig4: The inputs and the outputs of the parameter estimation method for a virtual tumor grown by reaction-diffusion modes are shown. Top row shows the tumor delineations as observed in medical images and also the

DT-MRI image of the subject. Bottom row shows the outputs of the method. The white contours are the tumor delineations observed in the images, the red contours are the evolution of the tumor delineation simulated by the traveling time formulation with optimized parameters.

Fig5: Example of an extrapolated image for a synthetic tumor. (Left) The image of a synthetic tumor is shown, where the white region is the visible part. The not-imageable infiltration region is also shown in color (from white=high density to green=low density). (Middle) The low density infiltration extrapolated by the proposed method starting from the visible part. (Right) Iso-density contours of the actual distribution (red solid) and the corresponding ones of the extrapolated distribution (white solid). The black contour is the tumor delineation visible in the image. We observe the high global resemblance.

Fig6: The proposed variable irradiation region construction takes into account the growth dynamics of the tumor. Figure shows the two irradiation margin construction approaches and the synthetic tumor cell distribution they aim to target. Figure (Left) cell distribution of the synthetic tumor. The white region is the visible part while the colored region is the infiltration not visible in the image. Figures (Middle) and (Right) show constant and variable irradiation regions overlaid on the tumor distribution respectively. Blue regions represent the areas to be irradiated. For the synthetic tumor the variable margin better covers the extent of the infiltration therefore provides a better targetting.

Fig7: The parameter estimation method is applied to the images of a real patient suffering from high grade glioma. Images in columns (Left column) and (Middle column) shows different slices of the T1-post gadolinium images which are used to estimate the parameters of the growth model as: ρ=0.05/day (set), d_w=0.66 mm^2/day, d_g=0.0013 mm^2/day. In (Middle column) we also show the manual delineation of the tumor (in white) used in parameter estimation along with the optimum simulation obtained by the estimated parameters (in black) (only white contour is shown in (Left column) since it is the same as the black one). (Right column) The final image shows the final state of the tumor and the evolution of the delineation predicted by the estimated parameters as the black contour. The figure is Copyright © 2009 IEEE.

Fig8: As a second case we applied our methodology to the images of a patient suffering from a low grade tumor. Images (First three columns) show different slices of the T2 flair images and the manual delineations (in white) which are used to estimate the parameters of the growth model as: ρ=0.008/day (set), d_w=0.20 mm^2/day, d_g=7x10^{-4} mm^2/day. Also in these images we show the simulated evolution of the tumor delineation obtained by the estimated parameters in black contours. The simulated evolution starts from the white contour in the Image (Left column). Images (Right column) are the slices of the final image showing the final state of the tumor and the delineation predicted by the estimated parameters as the black contour. The figure is Copyright © 2009 IEEE.

Fig9: For an example virtual tumor we plot the R vs. time (Left) and Vol. vs. time plots (Right). Each time point corresponds to an image taken in the study as explained in Section 3.2 We see that potentially variable irradiation margins can improve the accuracy of irradiation margins.

Figures & Tables
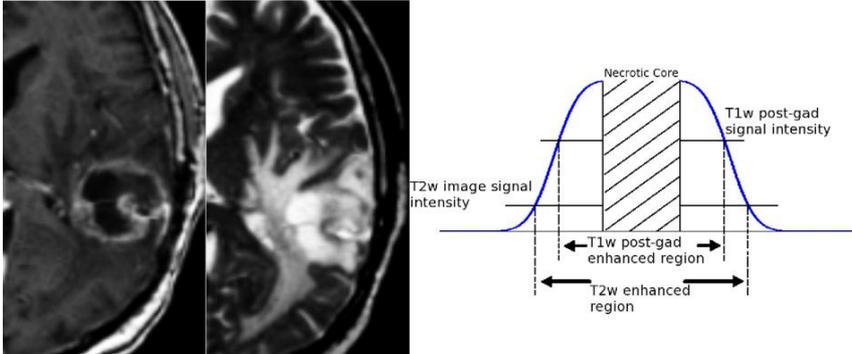
Figure 1
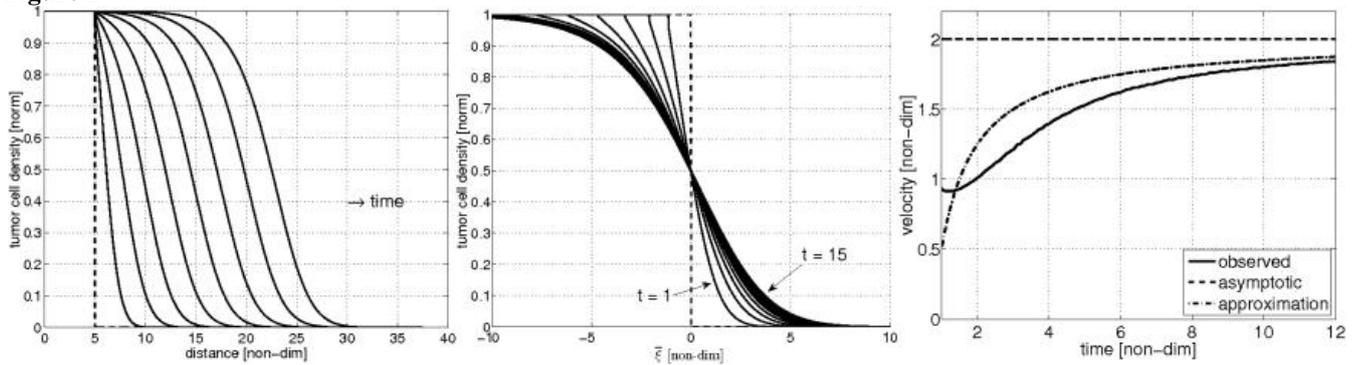
Figure 2
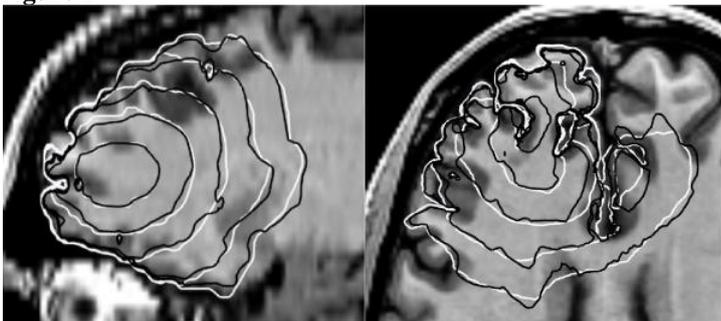
Figure 3
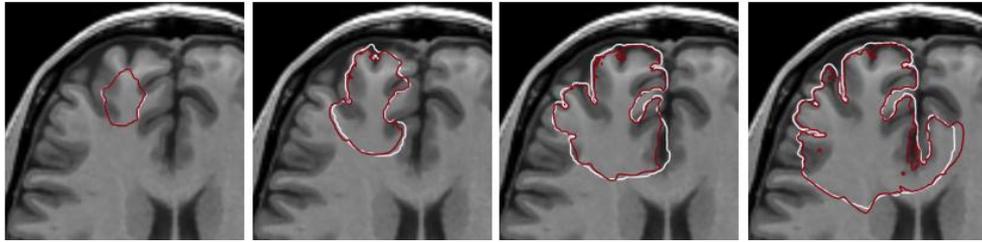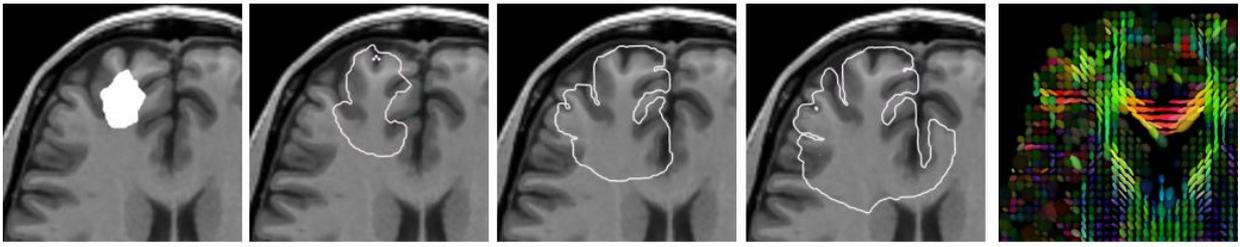
Figure 4
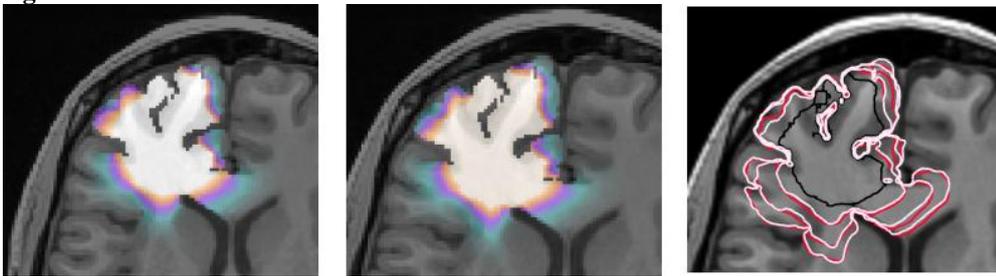
Figure 5
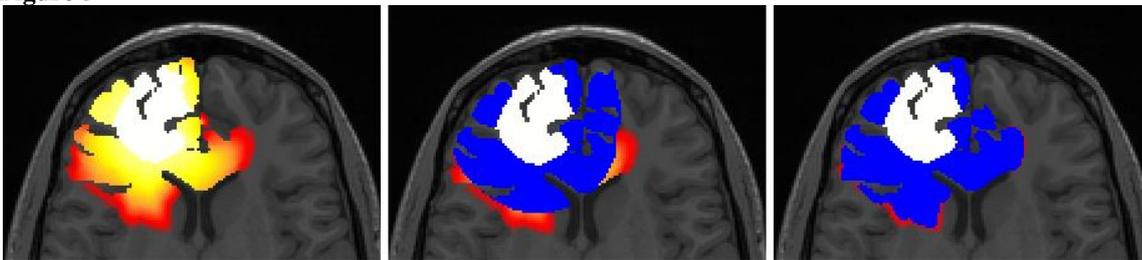
Figure 6
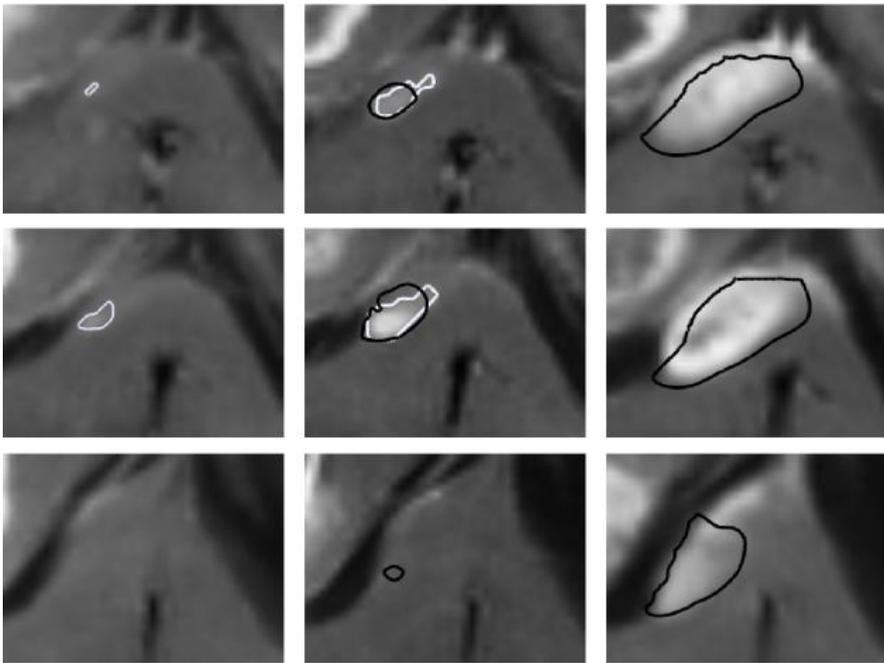
Figure 7

Figure 8

Figure 9